



#360

IMP-I

SUMMARY SPECTRA DATA

71-019A-15C



IMP-I

SUMMARY SPECTRA ON MAG TAPE

71-019A-15C

This data set has been restored. There was originally
1 Binary 9-Track, 1600 BPI tape. There is one restored tape.
The DR tape is a 3480 cartridge and the DS tape is 9-track, 6250 BPI.
The tape was created on an IBM 360 computer. The DR and DS number
along with the corresponding D number and the time span is as follows:

DR#	DS#	D#	FILES	TIME SPAN
DR03006	DS03006	D27597	3	04/20/71 - 09/26/72

REQ. AGENT

CMP

RAND NO.

RC6828

ACQ. AGENT

CDW

IMP-I

SUMMARY SPECTRA DATA

71-019A-15C

This data set catalog consists of 1 magnetic tape. The tape is binary, 9-track, 1600 BPI with a standard label and contains on file of data. This tape was created on an IBM 360 computer.

<u>D#</u>	<u>C#</u>	<u>LABEL</u>	<u>TIME SPAN</u>
D-27597	C-18427	Y1101	04/20/71 - 09/26/72

This document describes the basic data set compiled from the Goddard Space Flight Center radio astronomy experiment on IMP-6 (Explorer 43). The IMP-6 spacecraft was launched into a highly elliptical orbit (eccentricity of 0.94, 206000-km apogee, 354-km perigee, 4.18-day period) on March 13, 1971. The IMP-6 spacecraft was spin-stabilized with the spin axis oriented toward the South ecliptic pole and a spin rate ~ 5.5 RPM. The Goddard radio astronomy experiment operated from 13 March 1971, to 26 September 1972. The antenna used by the Goddard experiment was fully deployed on April 20, 1971, and the basic data set covers all measurements from that date until the end of the experiment lifetime (orbits 10 through 136). During this period radio measurements of the cosmic noise background and of a variety of transient sources in the solar system were obtained at frequencies between 30 kHz and 10 MHz. A description of the experiment has been published by Brown (1973), and a complete bibliography of all papers published on the results of the Goddard radio astronomy experiment is attached to this document.

The Goddard radio astronomy experiment (Fig. 1) used a 91-m dipole antenna which was comprised of two colinear, 46-m, X-axis (i.e. perpendicular to the spin axis) monopoles connected to individual wide-band high-impedance preamplifiers. The preamplifier outputs were combined in an electronic balun/power-splitter and then fed to two step-frequency, total-power radiometers. Each receiver sampled 32 discrete frequency channels once every 5.11 sec. Receiver 1 (SFR-1) operated between 30 kHz and 9.9 MHz with a crystal-controlled IF

bandwidth of 10 kHz and a post-detection integration time constant of 6 ms. Receiver 2 (SFR-2) operated between 30 kHz and 4.9 MHz with a crystal-controlled IF bandwidth of 3 kHz and post-detection integration time of 40 ms. The individual receiver channel frequencies are listed in Table 1. Each receiver had a total dynamic range of 60-dB which was divided into two 30-dB ranges in order to provide good ($\pm 3\%$) amplitude resolution.

In-flight calibration was automatically performed by injecting a sequence of four noise levels (two in each receiver range) from a calibration noise source in place of the antenna signal every 2.9 hr. The long-term drift in receiver gain determined from these data was approximately - 0.5 dB during the first six months of the flight and - 1.5 dB after 16 months of operation.

The most serious instrument performance problem encountered was due to saturation level signals at the pre-amplifier input which resulted in the generation of intermodulation products in the RF amplifiers which then appeared as wide-band signals in the telemetered data. This problem was most acute when intense kilometer wavelength emissions from the terrestrial magnetosphere were observed at frequencies in the 200-300 kHz range. An example of an event with significant intermodulation interference artifacts is shown in Figure 2.

Daily dynamic spectral plots were generated using the first 28 frequency channels of SFR-2 in the following fashion. For every 10-minute interval of data, signal intensity distributions, $N(I)$, were calculated at each frequency by sorting the data in 1-dB bins. Then the values of the mean, minimum, and maximum signal levels as well

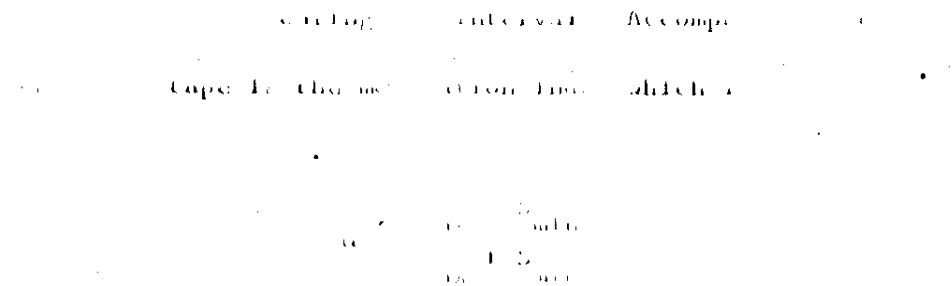
as the mode (most common value) of the distribution were determined for each 10-min interval at each frequency. These data were used to generate four 24-hr dynamic spectral displays which showed the variation of the average, minimum, maximum and mode of the received noise as a function of frequency and time with 10-min resolution. The intensity scale was plotted in increments of 1 dB with respect to the average background level at each frequency determined from studies of the long-term baseline level. The display format is illustrated and explained in Figures 2 and 3.

The dynamic spectral plots discussed above were generated from data contained on the IMP-6 Ten Minute Summary Tape. The contents and format of that tape are described in the appendix. In addition to the average, minimum, maximum and mode, the Ten Minute Summary Tape contains the average direction of arrival of emission at each frequency. The arrival direction was determined from the modulation pattern impressed on the data by the 5.5 RPM spin of the dipole antenna. The computation of the arrival direction was simply a Fourier fit to the data of a function proportional to $1 + \alpha \cos 2(\omega t - \phi)$ where the spin period, $1/\omega$, was precisely known, and the phase angle ϕ and level of modulation α were unknown. The Fourier fit was usually done with 12 consecutive 5.11-sec samples. The derived phase angle was then converted into a solar elongation angle, ϕ , in the ecliptic plane with minus to the East and plus to the West. (Since the dipole pattern is symmetrical, the deduced arrival directions have a 180 degree ambiguity.) The 12-sample processing window was then slid forward one sample and a new Fourier fit was done. The arrival

directions characterizing each ten-minute interval are averages of the individual Fourier fits during the interval. Accompanying each arrival direction on the tape is the modulation index which is defined as

$$\alpha = \frac{s_{\max} - s_{\min}}{s_{\max} + s_{\min}}$$

where S_{\max} and S_{\min} are the maximum and minimum power flux predicted by the best-fit $\cos^2\theta$ modulation pattern during the processing window. Nominally α ranges from 0 to 1, but due to effects such as the use of a limited number of samples and the over-simplified assumption of constant source flux during the sample window, it often ranges from 0 to 1.5 in actual practice. The modulation index is a measure of either the size of the emitting source or its ecliptic latitude. Figure 4 shows how these quantities are related for a source of uniform surface brightness. An exhaustive discussion of the spin modulation analysis technique has been given by Fainberg (1976).



and to whom the Chinese have sold their power. Then consider the following points during the process:

- From 0 to 1, by the coffee break example, of the overall project approach, the main task is often from 0 to 1.
- From 1 to 4, especially the first two or three steps, the Chinese have sold their power.
- From 4 to 5, the Chinese have sold their power.

TABLE 1. IMP-6 GODDARD RECEIVER FREQUENCIES

CHANNEL	SFR 1	SFR 2	CHANNEL	SFR 1	SFR 2
1	30 kHz	30 kHz	17	600 kHz	600 kHz
2	44	44	18	737	737
3	55	55	19	870	815
4	67	67	20	1030	950
5	83	83	21	1270	1030
6	92	92	22	1450	1100
7	110	110	23	1850	1270
8	130	130	24	2200	1450
9	155	155	25	2600	1630
10	185	185	26	3250	1850
11	210	210	27	3930	2200
12	250	250	28	4900	2600
13	292	292	29	5700	3000
14	375	375	30	6870	3600
15	425	425	31	8300	4200
16	475	475	32	9900	4900

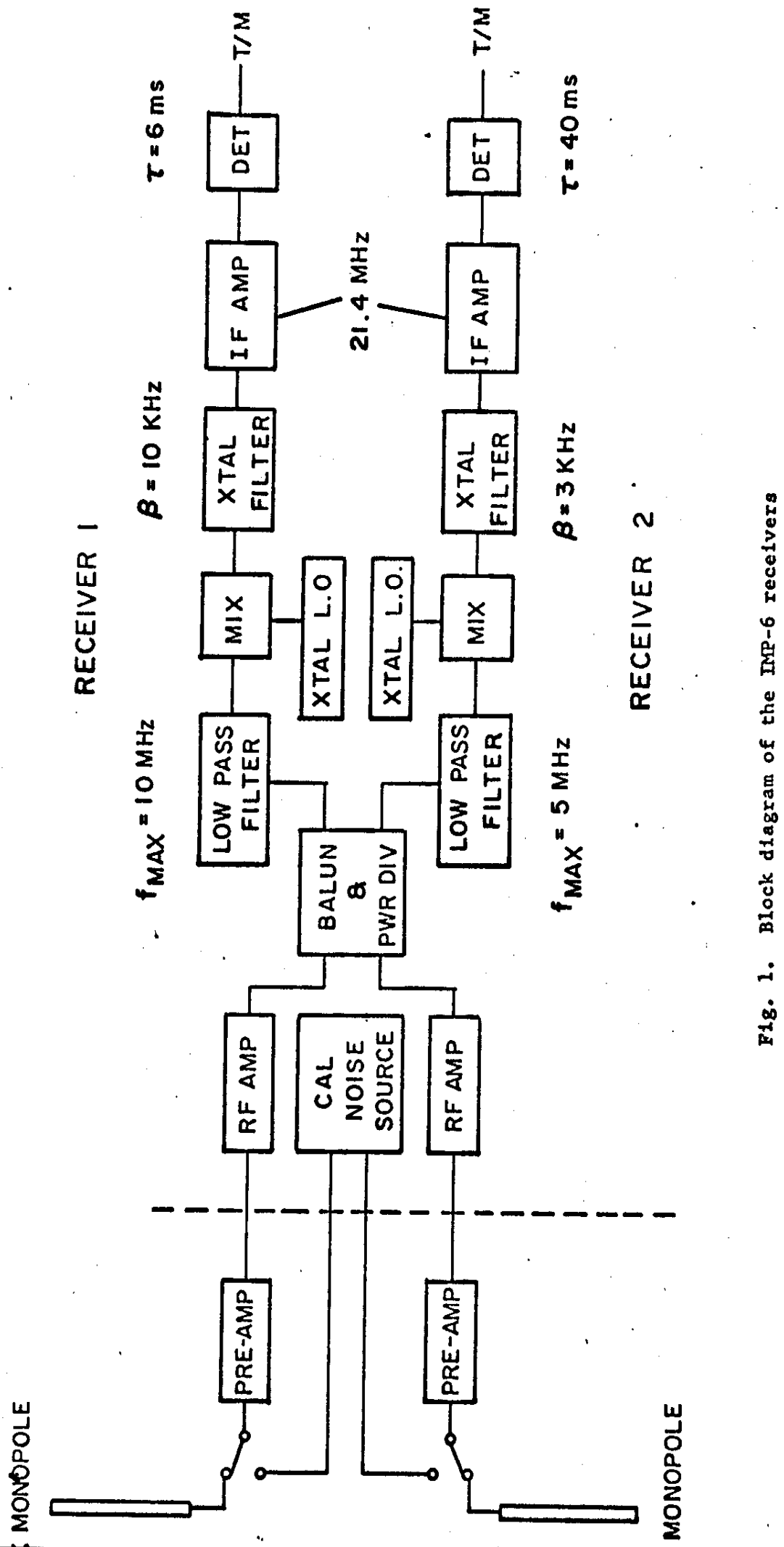


Fig. 1. Block diagram of the IMP-6 receivers

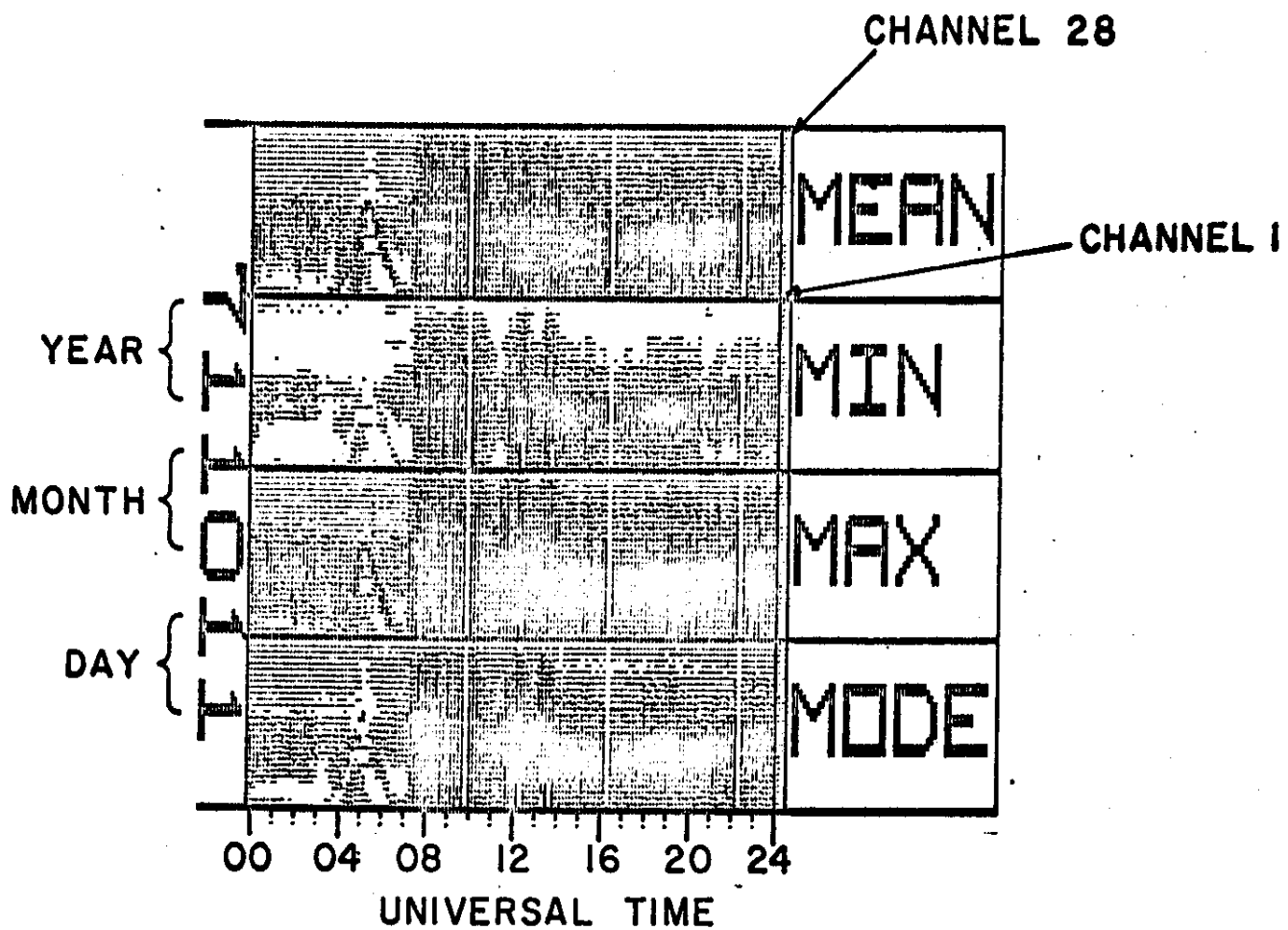


Fig. 2. Twenty-four hour dynamic spectrum in which increasing darkness indicates increasing intensity. The vertical "stripes" which appear after 7 hr are due to intermodulation effects in the pre-amplifier caused by intense terrestrial noise levels at frequencies near 0.3 MHz (frequency channels 7-15). The event between 04 and 07 hr resembling an arrowhead is the upper-hybrid resonance noise near perigee reported by Mosier et al. (1973).

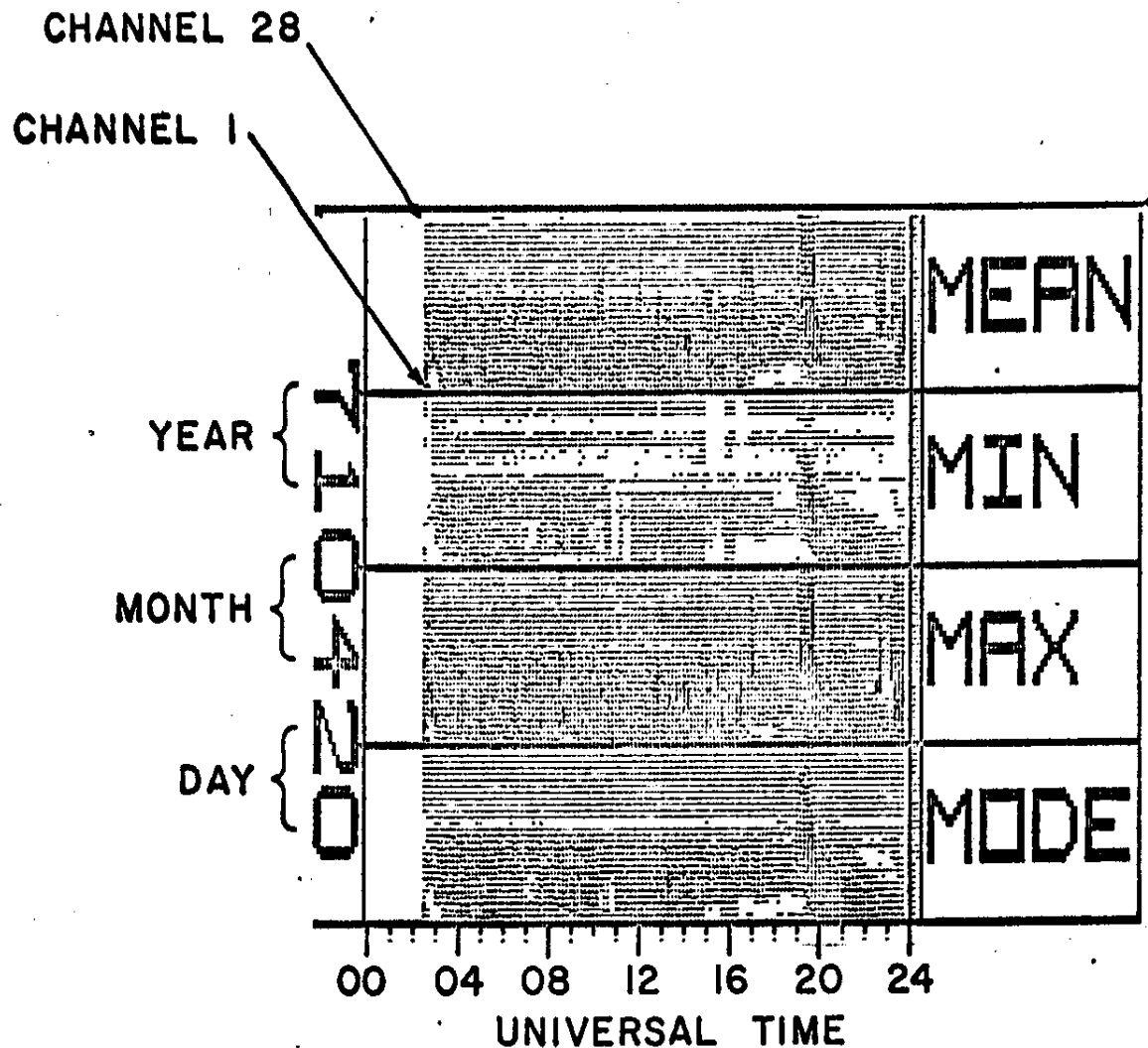


Fig. 3. Both this figure and Fig. 2 are examples of the dynamic spectral displays generated from the IMP-6 Ten Minute Summary Tape. Increasing darkness indicates increasing signal intensity. Note (1) a type III solar radio burst at about 19-20 hr, (2) weak terrestrial kilometer wavelength emission throughout the day, but particularly at 13-17 hr, and (3) interference from the NASA range and range rate tracking system at 23-24 hr. The range and range rate interference was particularly common during the first month of operation and can be easily recognized by its abrupt onset and sharp low-frequency limit of about 150 kHz.

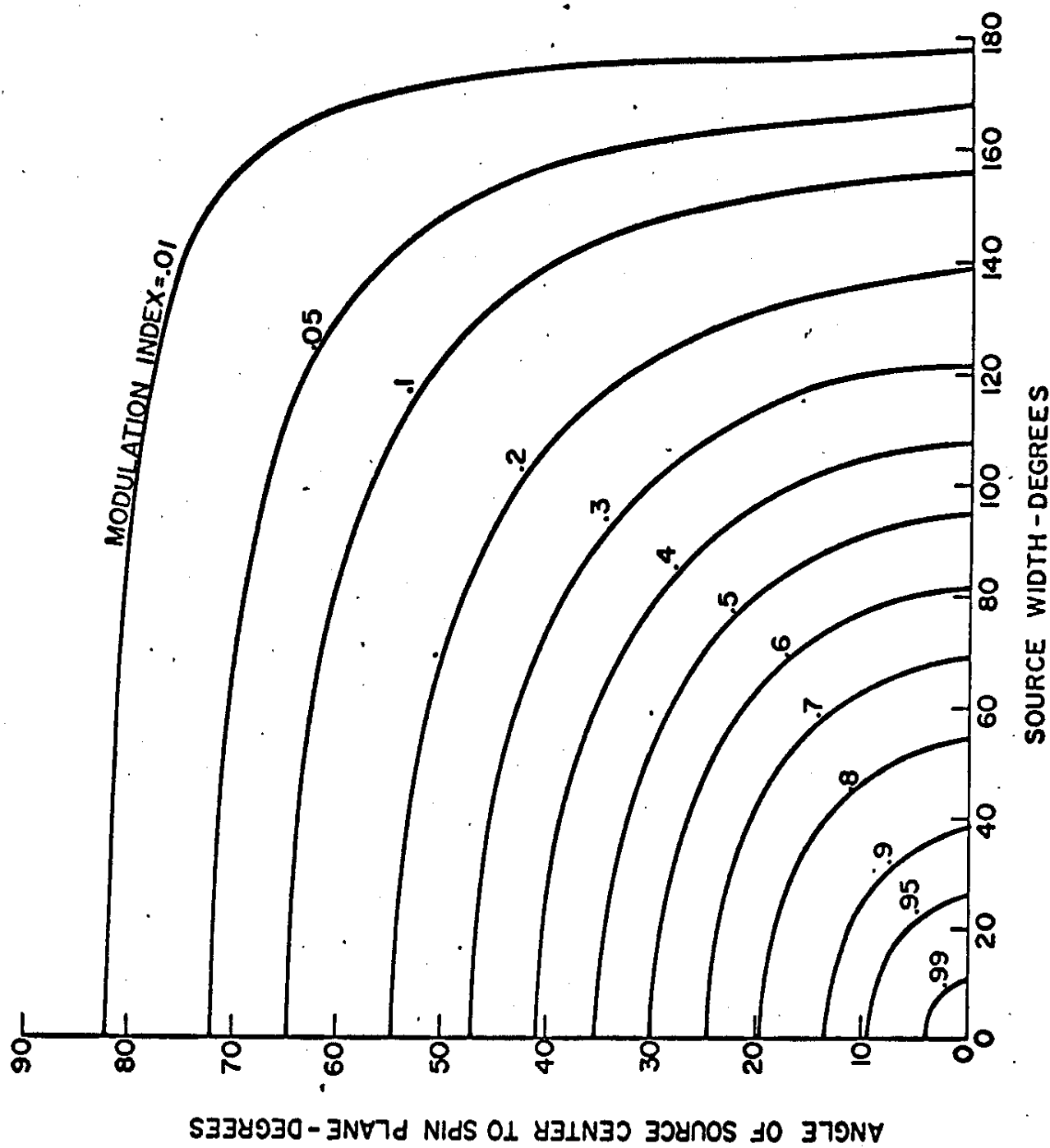


Fig. 4. The relationship between modulation index, source size and angle out of the spin plane (ecliptic plane) for a source of uniform surface brightness.

Appendix

TAPE FORMAT FOR THE IMP-6 TEN MINUTE SUMMARY TAPE

EACH LOGICAL RECORD CONTAINS A SUMMARY OF TEN MINUTES OF DATA FROM THE SFR-2 RECEIVER (FIRST 28 CHANNELS). THE TEN MINUTE INTERVALS ARE DEFINED TO START AT PRECISELY 0 HIR ON EACH DAY. THE LOGICAL RECORD LENGTH IS 416 8-BIT BYTES + A 4-BYTE LOGICAL RECORD CONTROL WORD. THE PHYSICAL RECORDS ARE 32344 BYTES (=420*77+4). THE TAPES ARE 2-TRACK 1600 BPI.
THE INDIVIDUAL QUANTITIES IN EACH RECORD ARE:

FORTRAN WORD	TYPE	LENGTH BYTES	DESCRIPTION
1	I	4	DATE IN YYMMDD FORM (E.G. MAY 15, 1971=710515)
2	I	4	UT IN ELAPSED SECONDS FROM 0HR AT THE START OF TEN MINUTE INTERVAL
3,4,5	R	4	GEOCENTRIC EQUATORIAL X, Y, Z OF SPACECRAFT (KMD)
6	R	4	SPIN PERIOD IN SECONDS
7-20	I	2	THE AVERAGE ANTENNA TEMPERATURE FOR THE FIRST 28 FREQUENCIES OF SFR-2 IN THE ORDER OF TABLE 1 THE AVERAGES ARE IN THE FORM 100*ALOG10(TAVE)
21-34	I	2	THE STANDARD DEVIATION OF THE AVERAGE ANTENNA TEMPERATURES ALSO IN THE FORM 100*ALOG10(TSTD)
35-48	I	2	AVERAGE SOURCE DIRECTION FOR EACH FREQUENCY AS DETERMINED FROM SPIN MODULATION. STORED IN THE FORM 100*PHI (IN DEGREES RELATIVE TO SUN WITH - TO EAST AND + TO WEST).
49-62	I	2	STANDARD DEVIATION OF AVERAGE SOURCE DIRECTION ALSO IN THE FORM 100*PHISTD
63-69	I	1	NUMBER OF SAMPLES AT EACH FREQUENCY IN THIS TEN MINUTE INTERVAL
70-76*	I	1	2% MINIMUM ANTENNA TEMPERATURE IN DB ABOVE 1°K
77-83*	I	1	2% MAXIMUM ANTENNA TEMPERATURE IN DB ABOVE 1°K
84-90*	I	1	MODE (MOST COMMONLY OCCURRING) ANTENNA TEMPERATURE IN DB ABOVE 1°K
91-97	I	1	MODULATION INDEX FOR EACH FREQUENCY AS DEDUCED FROM SPIN MODULATION
98-104	I	1	STANDARD DEVIATION OF MODULATION INDEX

* THE 2% VALUES AND THE MODE WERE DETERMINED BY FORMING HISTOGRAMS (FOR EACH FREQUENCY) IN 1 DB INCREMENTS FROM THE INDIVIDUAL SAMPLES TAKEN DURING THE 10 MINUTE INTERVAL. THE HISTOGRAMS WERE THEN SCANNED TO FIND THE LOWEST BIN CONTAINING AT LEAST 2% OF THE TOTAL NUMBER OF SAMPLES, THE HIGHEST BIN CONTAINING 2% OF THE TOTAL, AND THE BIN CONTAINING THE MOST SAMPLES (MODE). IN SOME CASES, NO BIN CONTAINED AT LEAST 2% OF THE VALUES, SO A ZERO WAS WRITTEN ON TAPE.

THIS TAPE CAN BE READ AS FOLLOWS (IN IBM FORTRAN IV)

```

INTEGER*4 A(104)
LOGICAL*1 NUM(28),MIN(28),MAX(28),MODE(28),ALPHA(28),ASTD(28)
INTEGER*2 TAVE(28),TSTD(28),PHI(28),PHISTD(28)
EQUIVALENCE (A(1),IYMD),(A(2),ISEC),(A(3),X),(A(4),Y),
1 ((A(5),Z),(A(6),SPIN),(A(7),TAVE(1)),(A(21),TSTD(1)),
2 ((A(35),PHI(1)),(A(49),PHISTD(1)),(A(63),NUM(1)),
3 (A(70),MIN(1)),(A(77),MAX(1)),(A(84),MODE(1)),
4 (A(91),ALPHA(1)),(A(98),ASTD(1)))

```

```
READ(IUNIT,END=XXXX) A
```

p. 11

IMP-6 GODDARD RADIO ASTRONOMY EXPERIMENT BIBLIOGRAPHY

1972

Fainberg, J., L.G. Evans, and R.G. Stone, "Radio Tracking of Solar Energetic Particles through Interplanetary Space", Science, 178, 743-745, 1972.

1973

Brown, L.W., "The Galactic Radio Spectrum between 130 and 2600 KHz", The Astrophysical Journal, 180, 359-370, 1973.

Evans, L.G., J. Fainberg, and R.G. Stone, "Characteristics of Type III Exciters Derived from Low Frequency Radio Observations", Solar Physics, 31, 501-511, 1973.

Lin, R.P., L.G. Evans and J. Fainberg, "Simultaneous Observations of Fast Solar Electrons and Type III Radio Burst Emission Near 1 AU", Astrophysical Letters, 14, 191, 1973.

Malitson, H.H., J. Fainberg, and R.G. Stone, "Observations of a Type II Solar Radio Burst to 37 R", Astrophysical Letters, 14, 111-114, 1973.

Malitson, H.H., J. Fainberg and R.G. Stone, "A Density Scale for the Interplanetary Medium from Observations of a Type II Solar Radio Burst out to 1 Astronomical Unit", The Astrophysical Journal, 183, L35-38, 1973.

Mosier, S.R., M.L. Kaiser, and L.W. Brown, "Observations of Noise Bands Associated with the Upper Hybird Resonance by the IMP-6 Radio Astronomy Experiment", Journal of Geophysical Research, 78, 1673-1679, 1973.

Stone, R.G., "Radio Physics of the Outer Solar System", Space Sciences Reviews, 14, 534-551, 1973.

1974

Brown, L.W., "Jupiter Emission Observed near 1 MHz", The Astrophysical Journal, 192, 547-550, 1974.

Brown, L.W., "Spectral Behavior of Jupiter near 1 MHz", Astrophysical Journal (Letters), 194, L159-L162, 1974.

Fainberg, J. and R.G. Stone, "Satellite Observations of Type III Solar Radio Bursts at Low Frequencies", Space Science Reviews, 16, 145-188, 1974.

1975

Brown, L.W., "Saturn Radio Emission near 1 MHz", The Astrophysical Journal, 198, L89-92, 1975.

Kaiser, M.L. and R.G. Stone, "Earth as an Intense Planetary Radio Source: Similarities to Jupiter and Saturn", Science, 189, 285-287, 1975.

Kaiser, M.L., "The Solar Elongation Distribution of Low Frequency Radio Bursts", Solar Physics, 45, 181-187, 1975.

1976

Brown, L.W., "Possible Radio Emission from Uranus at 0.5 MHz", Astrophysical Journal, 207, L209-L212, 1976.

Fainberg, J., "A Precise Method of Determination of Source Direction and Width from Spin-Modulated Spacecraft Measurements", GSFC Rept. X-693-76-91, 1976.

Fitzenreiter, R. J., L. G. Evans, and R.P. Lin, "Quantitative Comparisons
of Type III Radio Burst Intensity and Fast Electron Flux at 1 AU",
Solar Physics (in press; also GSFC Rept. X-693-75-236), 1976.

Fitzenreiter, R.J., J. Fainberg, and R.B. Bundy, "Directivity of Low
Frequency Solar Type III Radio Bursts", Solar Physics (in press;
also GSFC Rept. X-693-75-284), 1976.

RECORD 1 OF FILE 2
LENGTH = 32344 BYTES

Tmp.T

DATE

DATE	000002326	C3F78A8F	C42E88E3	43B984D1	41B203AE	04930436	05600548
03FF038E 039F0383	03520338	032602F0	037F03F7	02F802D2	02F902D0	02DF02DC	02D702D1
02CA02C4 02B502AF	048F044A	058B0587	043003A3	03AB03C5	0363035F	03FB0341	03TE02FD
033C02FF 02F802F9	030102FC	02F402FE	030202FC	02C102F0	0883116F	0DE1E1427	131C1390
099A18F2 0AAD1044	1C3E09A9	140000A7C	0A2109D2	09000738	02E90338	04B4021A	E6C5F841
12080EB3 0D220E42	06900540	0D9304E2	0740067C	06400681	0EBA1198	0A010563	090B02C6
018E0961 02D80608	0B68063A	0E551014	78785856	78787878	78787878	78787878	78787878
78787878 68656B65	4F4F564C	4C4A4742	42454545	47484849	48474746	46454443	70719594
50585A50 6500544C	4044AA49	484BAA49	484B6645	6F6A6250	5751594E	4D4CA846	45464747
49494847 47464544	19438251	42380133	2E1F40304	394A3A16	3D0F1215	140D0908	12231010
ID1F110 1C16210E	153D01311	31071414	03130304	11030106	01A40000	000AD714	00002500
C43A26B8 44143A4E	41822251	04E203E4	03D803D9	039F03A5	03850389	040103F4	03680374
03040320 02F102EA	02EF03AA	02E902E0	02D802F4	02C502BA	02F002A4	051E03CB	03E70388
03890393 04480428	038A0388	03A20329	03E035E	02F802F4	02F403F1	02F302F3	02F20317
031302F0 060F051C	05C1041B	075A063B	076905D8	01100E27	064904D9	0530565	062E0462
0470028A 037F0330	047602E8	03330586	038EFF8C	027605A2	026202C2	08790D45	0A500A5
0C660490 046A0484	03A40428	01EF0235	03D00643	02A40407	052705A2	049305F0	1C1C1C18
1C1C181C 1C1C1C1B	1B1C181C	1C1C1C1C	1A1C181C	1C1C1C1B	5F5C5B4F	5190544E	404F483C
3448433C 3A5A4342	2E40382D	6A676C6E	68646160	74770613F	6256545D	4F4C7E5C	4E4C4A54
6C655E58 58575750	52564D3C	47484A49	44A4A4A4	4A494847	47474544	182611921	302C2D2B
) 29232E21 2A292924	1F232017	12000808	0906071A	1C1D2018	10282909	0C9E00810	0E18120A
0A040604 01A40000	000AD714	0002D78	43607E7	444FC3C	441D9850	410303D9	03AB03AE
048104B2 040203DA	03ED03C4	033402F3	02EC02F2	03010304	03130308	030302F0	02EA02DA
02D202C8 02BD02B1	038503CA	038103B5	04A504D7	04520423	04280407	03680304	02FF0305
030E0307 03050300	02F93002	039102FC	02F702FC	030202FB	03D803B1	03FF0335	F9E40290
05E40405 056604EB	052F035A	030B01DF	02E1023B	05C4042B	055E0805	069F02D2	09AE031E
08810C92 0874161D	13930500	024703E7	02E40157	04320165	00E800E3	01700189	01730110
020F02F4 017404AD	030402D8	0DB70A40	78787878	78787878	78787878	78787878	78787878
78787878 615955A5	53525551	4E4B4A46	45484849	4A494949	49484847	46464543	66676664
6E6C584F 50505253	5352514F	504F504C	4A484746	636250D5	54545383	519304E3	4749A4B8
4A494948 47474544	22142010	5D22CF22	291C2A34	443C3635	3123161B	1717100E	12090905
13080307 08060705	06020308	09040608	05040103	05020601	01A40000	000AD714	00002A30
C44C5CDC 4424B538	41B22251	0403030E	03D90475	04C903C6	0374035F	03460324	03280311
030F0314 030A02F9	02F602EF	02EA02E6	02DE02D6	02CD02C7	02BD02B0	03E103C7	03BC0499
0320349 03310316	03200315	031802F9	02F70301	02ED02E7	02ED02F0	02EB02E6	02EB02A
02EF02EA FECFCFDD	08870104	02AA0718	056D0500	052304FC	04B045A	0487031C	03E4036C
07F4068F 07A007AA	0659059A	08490934	099A0697	0FB51147	00DCA0A69	0485501CE	01C70208
00ED00CD 01800184	01C201D8	020D020C	037F0416	02990445	02160270	078003E1	0D1C0C51
3C3C3C3C 3C3C3C3C	3C3C3C3C	3C3C3C3C	3C3C3C3C	635E5E62	605B5651	4F4C4A48	4849494A
4AA9A949 49A8A8A7	4645A543	6A676678	81655A5A	57545554	55505052	524EA4E4D	ACACAAA9
65619362 61605855	524E5049	404B504D	484B504A	49494948	47474544	182C191C	0B121E36
33272420 101A1817	14130F110	10080804	10261219	1030404E	06040505	09060505	03070404
0F030402 01A40000	000AD714	00002C80	441C2FDF	C45461F2	442D25E6	01622251	04710433
03D503E9 03A503DE	03C60375	035F0347	032B02FC	02FB02FB	02F502F2	02F202EB	02E702E4
02CF02C5 02BC02B0	04B0040B8	048A044A	0388B03D3	038A030B	03CE035B	033C0329	03120301
03010300 030102FE	02F002F1	02FE02FF	02FE02F8	030102FC	DEE505D0	04C001DC	07E50855
05280407 05E40584	06E60612	03A504FF	0650066C	062E050D	062B050DA	07330887	08350A0D
05301027 04250030	06C00724	06C00694	06E60686	075107F8	06D0407F8	0686064	06D90746
068606E8 06B8080F	088C0877	0AD50F77	78787878	78787878	78787878	78787878	78787878
78787878 6261615C	605F5959	5552514E	4C494949	49494949	42484747	46454443	7E827A74
67585856 544F4F4E	4D4D4E4E	48484745	54484745	54484745	54484745	54484745	54484745
4A494948 47464544	3D100E05	1119222F	35303130	232B2822	101C1C18	15191208	1C140903
03050309 06060607	080A080D	080C0A08	04070504	04040502	01EA0400	000002E0	44256026
C4595EE 44334037	4B22251	0480428	03D0381	03F042F	03E042E	03D0349	032D0305
02FF02F2 02F402F4	02540254	02B70258	02E70258	02E70258	02E70258	02E70258	02E70258
03BF0409 031F9035	0342032A	03670306	02670306	02670306	02670306	02670306	02670306

RECORD 932 OF FILE 2
LENGTH = 3234 BYTES

7E580000	01740000	00080010	0000FD20	452EE5C2	449F7928	41C8E394	03F03E1	03A00362
033A032C	034102F4	03000345	034F02F1	032F0329	03240326	02DC02D5	02D302CC	02D902C1
02B902B2	02A002A3	030003A3	037D0328	03000302	031A0300	02FF0323	03590306	0326033E
02FE02FB	02F50301	02FD02F9	02FC02FB	030402FF	FF8BF6D1	FEB3FF74	FE9CFD68	0051FE8B
FD880043	00A00FCD8	FC51FB08	FF13FA55	FF130090	0184017C	00DC00A4	0267016B	FE5D0177
02AA0A29	02B205A2	055F0680	03A501EF	021D0233	02590261	050F02FF	03450537	032802B0
02FC02F	02F404AC	02F0DB8	78787878	78787878	78787878	78787878	78787878	78787878
78787878	62F16563	4F4FA43	494FA43	3F464748	46464646	47464745	44464645	5453554F
4F575851	59385C57	4C4A4A69	49464646	60635C56	5250534A	4053544B	464D604C	48424448
4E474846	45454443	18152115	16172343	3B34625F	564A4F3B	1D181716	10160A0B	12090707
08090809	070B0E0A	1B0E1217	0E050A0A	03090402	07030304	01A40000	0008001D	000FFF78
4475F3FF	449E9A3A	41C8E776	03F903DC	0393035E	03380327	034002FC	03020331	02F102D8
032D0321	02D902D5	02D602D2	02D302CC	02E502C1	02AB02A4	02C203AD	035C032D	030D02FF
03160304	03040308	03050302	03BD0346	0338032A	02FF02F8	03000304	02F902F8	030002F9
02FB02FF	018BF05F	FC31FC83	FE34F8FA	FEAOFDFA	FD3FFFC3	FF82FCED	F9C8FA0	FB37FC35
00A4021B	01670080	00CA0249	05440002	0054FA50	07110339	02D8047D	04E0052A	03360221
02480320	07620344	02A20381	03680316	06520602	03C2061A	04E3035D	0E3F04F8	09530C59
78787878	78787878	78787878	78787878	78787878	78787878	635F5851	4FAD4F43	454FA430
46464646	47464745	44444340	67655D58	54525550	50535150	64595857	4B49A4A9	49484A47
66625C56	5265034A	4D24941	464DA4A8	49484848	48474846	45454443	181C191C	181C191C
55535330	16171915	06140A08	12046066	06046056	0808070C	0D080A0E	09050A05	09121015
08030303	01A40000	0008001D	000101D0	452EEFC01	4A2713D0	0A9D8A88	A1C86A88	A1C86A88